

Diurnal variability of size-differentiated inorganic aerosols and their gas-phase precursors during January and February of 2003 near downtown Mexico City

Mireya Moya*, Michel Grutter, Armando Báez

Centro de Ciencias de la Atmósfera, UNAM, Ciudad Universitaria, 04510 Mexico City, Mexico

Received 12 January 2004; accepted 31 May 2004

Abstract

Size-differentiated atmospheric aerosol particles along with gas-phase precursors were measured at a site near downtown Mexico City (MER site) during January and February 2003 to provide information regarding the diurnal variability and partitioning of semi-volatile inorganic compounds between the gas phase and different-size particles. The aerosols were sampled with cascade impactors (MOUDI's) in the following periods: 1st (06:00–09:00 h, LST), 2nd (09:00–12:00 h, LST), 3rd (12:00–15:00 h, LST) and 4th (15:00–18:00 h, LST). The gas-phase measurements were continuously recorded with an open-path FTIR spectrometer. Overall, inorganic aerosol size/composition measurements observed a bimodal distribution: one mode was present in the accumulation size range (0.18–0.32 μm , aerodynamic diameter) and the other in the coarse mode (over 1 μm , aerodynamic diameter). During the morning sampling periods, the highest concentrations occurred mainly over the accumulation mode while during the afternoon sampling periods, concentration peaks were observed over both accumulation and coarse modes. More than half of the ammonium was found in the accumulation mode. The rest of the ions (sodium, chloride, sulfate, nitrate, calcium and potassium) were prominent in both modes. The significant presence of sodium and crustals (calcium and potassium) are explained in terms of the potential influence of the dry salt-lake of Texcoco and resuspended dust/soil, respectively. Based on the analysis of the time-resolved PM and gas-phase composition, the significant presence of gas-phase ammonia (> 35 ppb) during the morning sampling periods was of importance in neutralizing the aerosol particles.

© 2004 Elsevier Ltd. All rights reserved.

Keywords: Atmospheric aerosols; Gas-phase precursors; Aerosol partitioning; Mexico City

1. Introduction

Atmospheric pollution in the Mexico City basin due to high levels of particulate matter (PM) and ozone has become an issue for its nearly 20 million inhabitants (Molina and Molina, 2002). PM levels exceed the Mexican PM₁₀ (PM with aerodynamic diameter $\leq 10 \mu\text{m}$) 24-h standard on most days of the year (Edgerton et al., 1999). Although there is not a Mexican

standard for PM with aerodynamic diameter $\leq 2.5 \mu\text{m}$, the PM_{2.5} levels in the valley are routinely above the acceptable limits using as a reference the US 24-h average standard of $65 \mu\text{g m}^{-3}$. Knowledge of the size and chemical composition of aerosols is important to assess their role in several processes occurring in the atmosphere. For instance, visibility reduction, cloud formation, climate forcing and gas-particle interactions are affected by particle size and/or composition (Seinfeld and Pandis, 1998). Particles are also known to have adverse effects on human health (Spengler et al., 1990; Dockery et al., 1992, 1993) and it has been suggested

*Corresponding author.

E-mail address: mmoya@servidor.unam.mx (M. Moya).

that the particle size and/or chemical composition are also important in this respect (Schwartz, 1996). The main constituents of atmospheric aerosols are inorganic ions, carbonaceous material, crustal elements and water. The ionic composition of an aerosol determines to a large extent its acidic/basic characteristics, influencing the partitioning of semi-volatile compounds between the gas-phase and different size particles (Fridlind and Jacobson, 2000). Measurements of the chemical composition of size-resolved aerosols along with gas-phase precursors are essential to provide information regarding the aerosol partitioning between the gas and particulate phases and to validate aerosol models (e.g. Moya et al., 2001, 2002a).

There are no published data on the size-differentiated chemical composition of aerosols along with time-resolved measurements of gas-phase precursors for this megacity. The scarcity of information about Mexico City aerosols has motivated a field campaign during 10 days of the 2003 cold dry season at a site near downtown of the metropolitan area to study: (1) the diurnal variability in the chemical composition of size-resolved aerosols and their gas-phase precursors; and (2) the partitioning of measured inorganic aerosols for Mexico City conditions.

2. Experimental

2.1. Sampling site description

The measurements were done on the roof of a High School (~ 20 m above ground level) located in downtown Mexico City next to the atmospheric-monitoring station MER run by the City Government (19.38° N, 99.12° W, see Fig. 1). The parameters used in this study, such as wind data, relative humidity, temperature and NO_x concentrations, were taken from the monitoring station Merced. The site is surrounded by near heavily traveled, paved and curbed surface streets with light-duty vehicles and modern heavy-duty diesel buses (Edgerton et al., 1999). A major bus station (known as TAPO) is located ~ 500 m to the NE and the Mexico City International Airport (MCIA, see Fig. 1) is ~ 2 – 3 km E from the sampling site. The dry salt lake of Texcoco (see Fig. 1) covering an area of ~ 12 km², lies approximately 15 km NE from the sampling site. Although the lake covered an important area of the Mexico Basin in the late 1920s (120 km²) a dramatic reduction of the lacustrine system has been occurring since then because the urban sprawl has increased from 86 to 1200 km² in the period 1930–present (Jazcilevich et al., 2000). An important characteristic of downtown Mexico City is the high density of population which was reported as $\sim 14,000$ inhabitants per square kilometer in the year 2000 (INEGI, 2000).

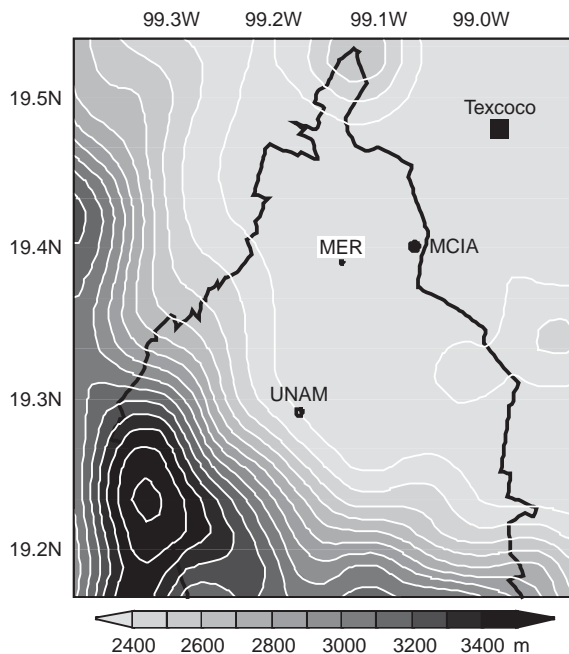


Fig. 1. The sampling site (MER) during the field study. Mexico City International Airport (MCIA), the Texcoco Lake and the University Campus (UNAM) are also shown in the figure.

2.2. Atmospheric conditions during the study

The nominal elevation of the Valley of Mexico is 2240 m above sea level. In spite of its elevation, Mexico City's location at 19° N latitude provides it with a temperate climate throughout the year. The climate was typically dry over the period of study (10 days in January–February 2003) with average relative humidity (RH) and temperature (T) of approximately 46% and 16°C , respectively. Although their diurnal trends were similar throughout the entire period, there was some variability from day to day. The ranges registered during the four sampling periods were as followed: 1st: 6.0 – 11.5°C and 63–77%; 2nd: 12.6 – 19.8°C and 27–48%; 3rd: 19.4 – 25.6°C and 19–41%; 4th: 19.0 – 25.7°C and 21–38%. As one can see from Fig. 2, winds were consistently coming from the NE during the 1st period and the more intensive ones (> 3 ms⁻¹) were registered from the ESE during the late afternoon (4th) period.

2.3. Urban air measurements

2.3.1. Particle collection

Size-differentiated particles were collected in 8-stage cascade impactors (MOUDI; Marple et al., 1991). Four periods of aerosol sampling (06:00–09:00 h, 09:00–12:00 h, 12:00–15:00 h and 15:00–18:00 h, LST) were conducted during each of the ten days of the study (28th

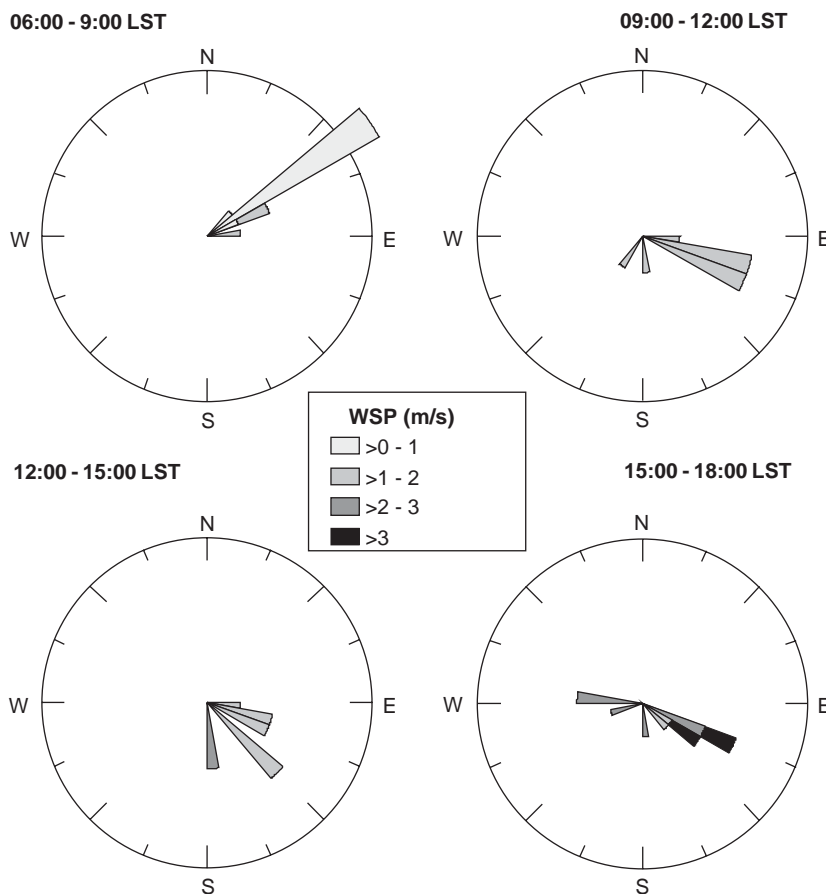


Fig. 2. Wind charts showing the prominent wind directions and intensities (grey scale) of the four sampling periods during this study. The radius axis represents the occurrence from 0% to 50%.

January through 7th February, 2003). For a continuous aerosol sampling a set of two MOUDI's were used. MOUDI (1) was collecting particles from the 1st and 3rd sampling periods while MOUDI (2) collected particles from 2nd and 4th sampling periods. The impactor flow rate was 30 l min^{-1} . The 50% cutoff in aerodynamic diameter for stages 1–8 was: 0.18, 0.32, 0.56, 1.0, 1.78, 3.16, 5.62, and $10 \mu\text{m}$, respectively.

A full description of the collection of size-resolved inorganic compounds (Cl^- , NO_3^- , SO_4^{2-} , Na^+ , NH_4^+ , Ca^{2+} and K^+) is presented elsewhere (Moya et al., 2003). Briefly, an aluminum foil (47 mm, MSP) was placed in each one of the stages of the MOUDI with an after-filter of quartz (37 mm, Pall-Gelman). All measurements were performed at ambient temperature and RH. Every aluminum filter was weighed before and after sampling on a semi-microbalance (Sartorius, Model MC210S) with a readability of 0.01 mg ($10 \mu\text{g}$). It should be noted that the particle loading in all cases was greater to 0.01 mg (which corresponds to $\sim 2 \mu\text{g m}^{-3}$, per impactor stage in 3-h MOUDI measurements). Before

weighing, the filters were conditioned for about 24 h in the weighing room at a RH of $40 \pm 5\%$ and at about 20°C . After sampling, the filters were stored in a cool ($+5^\circ\text{C}$), dark room until chemical analysis.

2.3.2. Gas-phase precursors

The gas-phase measurements for the present study were performed using an open-path Fourier Transform Infrared (FTIR) spectrometer. A full description of the experiment and location is presented elsewhere (Grutter et al., 2003). Briefly, an infrared beam is sent 426 m across the atmosphere using a bistatic telescope system. The IR radiation is modulated with a Nicolet[®] interferometer with 0.5 cm^{-1} resolution and captured with a HgCdTe detector at 77 K. The concentrations are retrieved from the 5 min co-added interferograms by performing a CLS regression using a synthetic background and references generated from the HITRAN spectroscopic database (Rothman et al., 1998). For the quantitative analysis of NH_3 and HNO_3 , the regions $920\text{--}1090$ and $875\text{--}900 \text{ cm}^{-1}$ are used, respectively. The

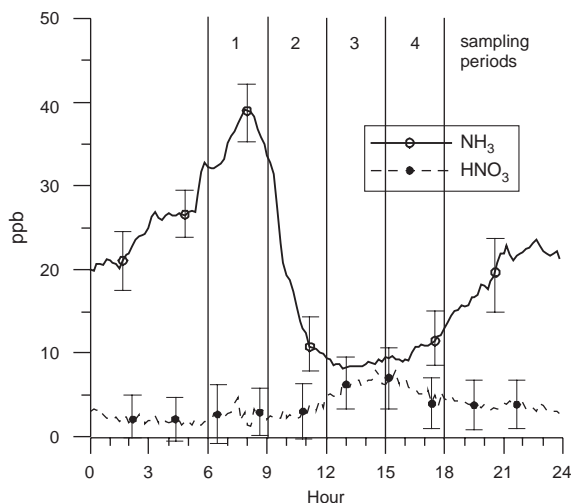


Fig. 3. Ammonia (NH_3) and nitric acid (HNO_3) diurnal profiles in parts-per-billion (ppb) from the open-path FTIR measurements for the entire period of this study. Sampling periods for the MOUDI samplers are marked with the vertical lines.

curves presented in Fig. 3 represent an average diurnal pattern of what was observed during this study. The error associated with the ammonia concentrations is between 15% and 20%, whereas that in the nitric acid determination is around 40%. Even if the uncertainty in the nitric acid determination is large due to its small fingerprint in the infrared, the relative increase in the afternoon periods can be clearly observed in the curve. Analysis of the spectra collected over the entire period indicates that the HCl concentration did not exceed the 2–3 ppb level.

2.4. Chemical analyses

Filter samples were kept in a petri dish and were ultrasonically extracted with 3 ml of deionized water in a beaker for approximately 60 min. Each extracted sample was made up to 5 ml. The inorganic ions (Cl^- , NO_3^- , SO_4^{2-} , Na^+ , NH_4^+ and K^+) were analyzed using ion chromatography (IC). Nitrate, sulfate and chloride were analyzed by non-suppressed IC, and ammonium, sodium and potassium by suppressed chromatography with a Perkin-Elmer chromatograph. A Hamilton PRP-X100 column was used for chloride, nitrate and sulfate analysis. The injection volume was 100 μl . The mobile phase was 2 mmol phthalic acid in 10% acetone and a flow rate of 2 ml min^{-1} . For ammonium, sodium and potassium ions, the injection volume was 50 μl . The analytical conditions were as follows: Hamilton PRP-X200 analytical column; Alltech 335SPCS suppressor module; Alltech cation suppressor cartridge. The mobile phase was a solution of nitric acid, 4 mmol in 7:3

(water:methanol) and 2 ml min^{-1} of low rate. Soluble calcium was determined by flame atomic absorption spectrometry using a GBC spectrometer. The aspirated volume during each analytical determination (considering a duplicate analysis) was 800 μl . According to the total volume of 5 ml (for each sample), we were able to make a replicate for each analytical determination (IC and atomic absorption spectrometry).

2.5. Experimental uncertainties

The analytical limits of detection for all ions (Cl^- , NO_3^- , SO_4^{2-} , Na^+ , NH_4^+ and K^+) determined by IC were in the range 1.1–5.0 neq ml^{-1} , which corresponds to air concentrations of about 1.6–7.0 neq m^{-3} (per impactor stage in 3-h MOUDI measurements). The analytical limit of detection for soluble calcium determined by atomic absorption (AA) was 0.5 neq ml^{-1} , which corresponds to air concentrations of about 0.7 neq m^{-3} (per impactor stage in 3-h MOUDI measurements). Overall, the concentrations of the ions determined by IC were sufficiently above the analytical limit of detection. On the other hand, the concentrations of Ca^{2+} in the lowest impactor stages (particle sizes $\sim \leq 0.56 \mu\text{m}$) were sometimes close to the analytical limit of detection, or within the variance of the measured blanks. The field blanks concentrations for anions (Cl^- , NO_3^- , SO_4^{2-}) were always below the lower detection limit (LDL) while for cations (Na^+ , NH_4^+ , K^+) were in the range of 3–9 μg . While these errors associated to chemical analysis tend to cancel out when averaging over a set of samples, other more systematic, such as the lack of volatilized nitrate measurements (Chang et al., 2000) do not and will be discussed in a subsequent section.

3. Results and discussion

3.1. Time-resolved gas-phase measurements

The curves presented in Fig. 3 represent an average diurnal pattern of what was measured during this study with the open-path FTIR spectrometer. Very high mixing ratios of ammonia (> 35 ppb) are present during the early morning sampling periods. The ammonia concentration then drops abruptly during the late morning sampling periods and remains at its low point throughout the afternoon periods. It is during these afternoon periods when the nitric acid presents a relative increase in its concentration. No HCl was observed above the detection limit throughout the field campaign, which is around 2–3 ppb for this open trajectory. The ammonia and nitric acid concentrations showed a regular day-to-day variation. The maximum was during the 1st sampling period (average at 7:40 h, LST) in the

case of NH_3 and in the afternoons (average at 15:00 h, LST) for HNO_3 . The average peak values and standard deviation were 44 ± 9 ppb for NH_3 and 11 ± 2 ppb for HNO_3 , presenting the highest values at 55.9 and 14.3 ppb during the entire period, respectively.

3.2. Average mass distributions

The average mass size distributions corresponding to each of the four sampling periods are shown in Fig. 4. As seen, two distinct modes, one in the accumulation and the other in the coarse mode, typical of urban aerosols (Seinfeld and Pandis, 1998), dominated the mass distributions. It should be noted that particle mass accumulates in smaller sizes, showing larger peaks during the morning sampling periods. Although not shown, the ionic fraction of the total mass was at most 50% for particles in the accumulation mode (particles $< 1 \mu\text{m}$) and 60% for particles in the coarse mode (PM larger than $1 \mu\text{m}$).

3.3. Diurnal variability of major inorganic ions

Figs. 5 and 6 show the average diurnal variability of chemical composition of major anions and cations, respectively. Overall, the inorganic aerosol size/composition distributions observed during all sampling periods of the study have two modes: one in the accumulation size range ($0.18\text{--}0.32 \mu\text{m}$, aerodynamic diameter) and other in the coarse mode (over $1 \mu\text{m}$, aerodynamic

diameter). The concentrations of major ions showed a more predominant peak over the accumulation mode during the morning sampling periods and over both accumulation and coarse mode during the afternoon sampling periods. Each mode has different formation pathways: Accumulation mode particles are likely the result from the condensation of secondary aerosol components from the gas-phase while coarse mode particles are primarily formed by mechanical processes (resuspension of dust or soil). As aforementioned, more intensive winds were registered from ESE during the afternoon sampling periods favoring the resuspension of dust/soil that seems to impact in the composition of coarse particles (see concentration of crustals, Fig. 6). Overall, chloride and sulfate were the dominant anions while sodium and in a lesser extent ammonium, were the dominant cations over all of the sampling periods of the study.

Ammonium was found in the accumulation mode ($\sim 0.32 \mu\text{m}$, aerodynamic diameter), predominantly during the morning sampling periods. Sulfate concentrations occurred prevalently over the accumulation mode ($\sim 0.18\text{--}0.32 \mu\text{m}$, particle size range) during the morning sampling periods and over both accumulation and coarse modes (~ 0.32 and $5.62 \mu\text{m}$, aerodynamic diameters, respectively) during the third sampling periods. In accord with the trend observed for NH_3 in the gas phase, there is a clear increase in the NH_4^+ content of the aerosol between the 1st and 2nd sampling periods, specifically $\sim 0.32 \mu\text{m}$, aerodynamic diameter (see

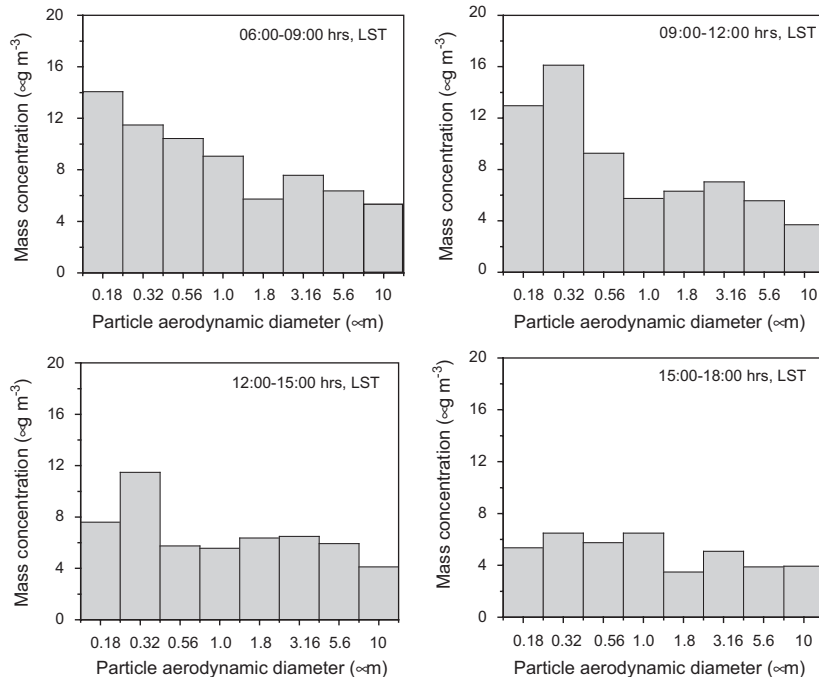


Fig. 4. Average particle mass distributions of major ions stratified by sampling period measured at the MER site.

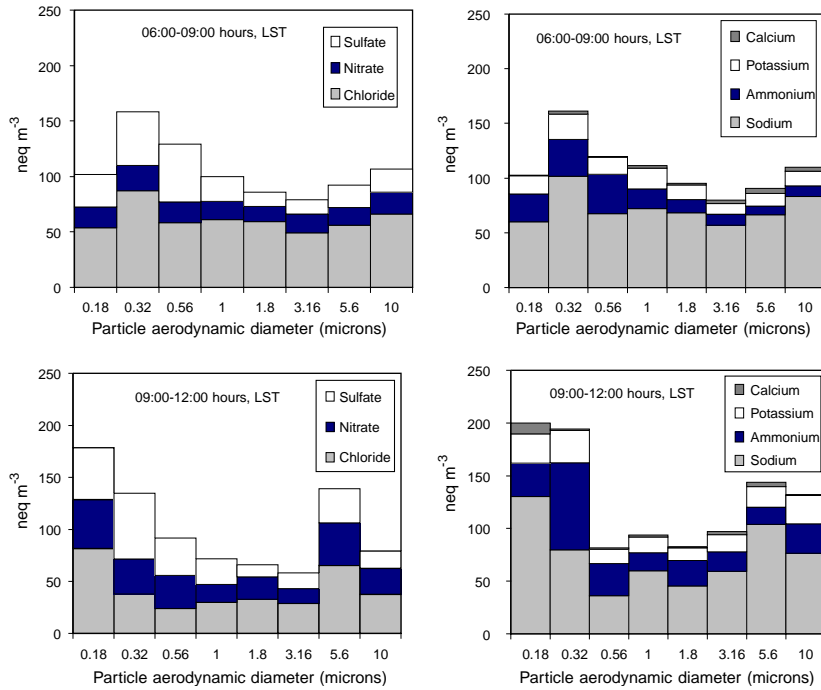


Fig. 5. Average size distributions of major ions measured at the MER site. Figures in the top correspond to concentrations measured during the first sampling periods (left, anions; right, cations). Figures in the bottom correspond to concentrations measured during the second sampling periods (left, anions; right, cations). Concentrations are given in nano-equivalents per cubic meter (neq m^{-3}).

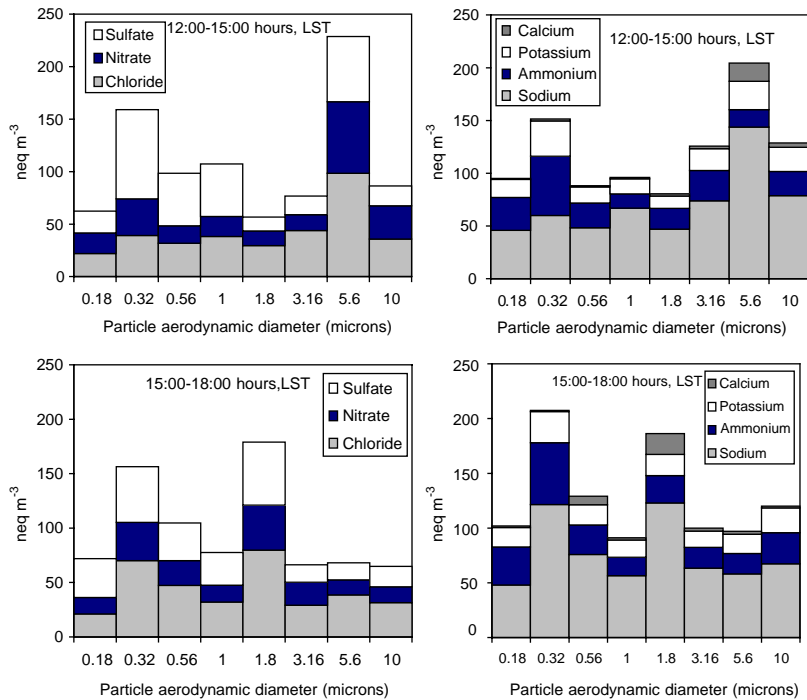


Fig. 6. Average size distributions of major ions measured at the MER site. Figures in the top correspond to concentrations measured during the third sampling periods (left, anions; right, cations). Figures in the bottom correspond to concentrations measured during the fourth sampling periods (left, anions; right, cations). Concentrations are given in nano-equivalents per cubic meter (neq m^{-3}).

Fig. 5). This neutralization process is favored, as shown in Fig. 7, with the lower temperature and higher RH values registered during the individual days. The plots in this figure also reveal that at lower availability of the gas-phase precursors (NH_3 and HNO_3), more NH_4^+ can be found in this accumulation mode thus suggesting the conversion from gaseous ammonia into the PM during this sampling period.

Nitrate, chloride, sodium and calcium were mainly found $\sim 0.18\mu\text{m}$, aerodynamic diameter, during the second sampling periods and $\sim 5.62\mu\text{m}$, aerodynamic diameter, during the third sampling periods. Potassium was found prevalently in the accumulation mode of all of the sampling periods. Sodium and chloride were correlated over all particle sizes and sampling periods. However, sodium concentrations were present mostly in 'excess' indicating the cation was possibly combined with other anions such as sulfate or nitrate. One possible source of sodium affecting the sampling site might be the dry salt-lake of Texcoco (Vega et al., 2001), which as aforementioned lies approximately 15 km NE of the measuring site (see Fig. 1). Re-suspended dust from the dry lakebed may affect the samples collected at this site

when wind direction is NE (Jáuregui, 1989), and Fig. 2 shows that the predominant wind direction during the morning sampling periods of the study was NE. Other sources for the observed coarse mode ions in Figs. 5 and 6 from the ESE to S are possible since the most intensive winds were registered from these directions during the 3rd and 4th sampling periods.

3.4. Relationship between NO_x , HNO_3 and particulate nitrate

Overall, the highest concentrations of NO_x (not shown) were observed during the early morning sampling periods (from 6:00 to 9:00 h, LST). During the afternoon sampling periods, NO_x concentrations were the lowest while the HNO_3 concentrations were the highest, suggesting this species serves as a sink for daytime removal of nitrogen oxides (Jacobson, 2002). Once HNO_3 is formed and start to increase in concentration (2nd sampling period), particulate nitrate is observed in moderate concentrations over the accumulation mode and during the afternoon sampling periods over the coarse mode. This coarse nitrate is

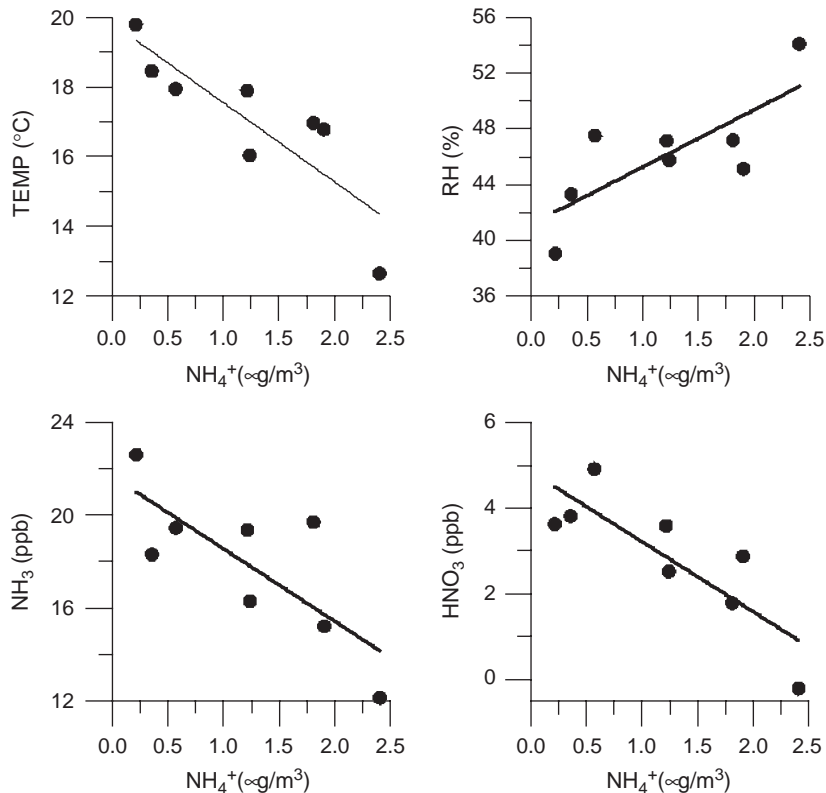


Fig. 7. Correlations of the ammonium ion found in the PM ($0.32\mu\text{m}$) during the 2nd (9:00–12:00 LST) sampling periods with respect to temperature, RH, gas-phase ammonia and nitric acid. Points not shown for two days correspond to values under the detection limit of NH_4^+ for this particular particle size.

probably a result of reactions of nitric acid with aerosol crustal material and/or sodium chloride (Fig. 6 shows the dominance in concentration of these chemical species). This interesting case, where secondary aerosol matter (nitrate) is formed through the reaction of a naturally produced material (dust, soil or salt from the Lake) and an anthropogenic pollutant (nitric acid), is in agreement with findings reported for several urban cities (see for instance, Wall et al., 1998). Fine nitrate is usually the result of the nitric acid/ammonia reaction for the formation of ammonium nitrate (Seinfeld and Pandis, 1998). It should be noted though, relative high temperature values (between 20 and 25 °C) observed during the afternoon sampling periods (3rd and 4th) seems to shift the ammonium nitrate equilibrium towards the gas phase (as shown in Fig. 3), in agreement with theory (Seinfeld and Pandis, 1998).

3.5. Size-resolved particles in the accumulation mode

3.5.1. Ion balances

Ion balances were performed over part of the collected aerosol samples in the accumulation mode to find out if sodium concentrations were combined with other anions (besides chloride), such as sulfate. The balances (Level II of data validation; Chow et al., 1994) were applied over samples collected at 0.18 and 0.32 μm , aerodynamic diameter, of the 2nd sampling periods and over samples collected at 0.32 μm , aerodynamic diameter, of the 3rd sampling periods where sulfate and/or ammonium concentrations were of relevance. Sulfate (as well as ammonium) often coexist in accumulation-mode particles because when sulfuric acid condenses, it usually prefers this mode as particles have more surface area, when averaged over all particles in the mode, than do nucleation- or coarse-mode particles (Jacobson, 2002). Two cases were examined over the samples under study: 'Case a' considers nitrate and sulfate or bisulfate are balanced by equivalent ammonium; and 'Case b' considers some of the sulfate is associated with sodium (Na^+) in an amount equivalent to the reduction of chloride (Cl^-) from its Cl^-/Na^+ ratio. For a detailed explanation of the type of ion balances performed in this work the reader is referred to Chow et al. (1994). Briefly, 'Case a' assumes that the entire particulate nitrate is in the form of ammonium nitrate and sulfate is either ammonium sulfate or bisulfate. Measured ammonium concentrations should equal those calculated from ammonium nitrate and ammonium sulfate or ammonium bisulfate on a molar-to-molar basis. In 'Case b' the ammonium balance is refined by subtracting sulfate, which might be present as sodium sulfate. This can occur by reaction of sulfuric acid with sodium chloride. If this is the case, the sulfate associated with sodium sulfate is subtracted as equivalent ammonium from the total calculated ammonium.

Figs. 8 and 9 show the ammonium balance for Cases a and b applied over the samples of the aforementioned aerosol particle sizes and sampling periods. As seen for Case a (shown in the left half of the figures) the majority of ammonium bisulfate points are on or closer to the one-to-one line with respect to the ammonium sulfate points. This suggests ammonium bisulfate is the dominant species. Since calculated versus measured ammonium concentrations are above the one-to-one line, this indicates that particles of these aerosol sizes are either more acidic (i.e. most of the sulfate is present as bisulfate or sulfuric acid) and/or particles are associated with cations other than ammonium, such as sodium.

Overall, by subtracting the calculated ammonium for sodium sulfate (Case b, shown in the right half of Figs. 8 and 9) shifts the points downward so the one-to-one line lies between the ammonium sulfate and ammonium bisulfate points. In the first example (0.18 μm , aerodynamic diameter, 2nd sampling periods) the scatter in the ion balance is reduced. This suggests the presence of sodium in this particle size range. For the second and third examples (0.32 μm , aerodynamic diameter, 2nd and 3rd sampling periods) the scatter in the ion balances is not reduced and this suggests sulfate be most probably combined with ammonium rather than sodium. In any case, ion balances show that for some cases under study sodium 'in excess' is combined with other anions besides chloride as expected.

3.6. Size-resolved particles in the coarse mode

The peaks of concentrations of sulfate and nitrate in the coarse mode ($\sim 5.6 \mu\text{m}$, aerodynamic diameter) are probably associated with sodium and/or crustal species. Nitrate is most probably combined with calcium through the called soil-particle acidification process, which occurs when nitric acid dissolves in soil-particle solutions containing calcium carbonate and water (Dentener et al., 1996; Jacobson, 1999). As aforementioned the lack of volatilized nitrate measurements in our study might introduce some errors in the size-differentiated nitrate concentrations reported here (Chang et al., 2000). These measurements are necessary to fully characterize and understand the partition of size-resolved inorganic aerosols in this megacity. The unexpected concentrations of potassium over both modes are explained by the potential influence of the dry salt-lake of Texcoco. Previous studies (Vega et al., 2001) have pointed out the significant enrichment of potassium, sodium, chloride and magnesium in samples taken at the dry lake. The presence of sodium and crustal species at the research site suggests their inclusion is important in characterizing Mexico City size-resolved aerosols in agreement with findings reported by Moya et al. (2002b, c).

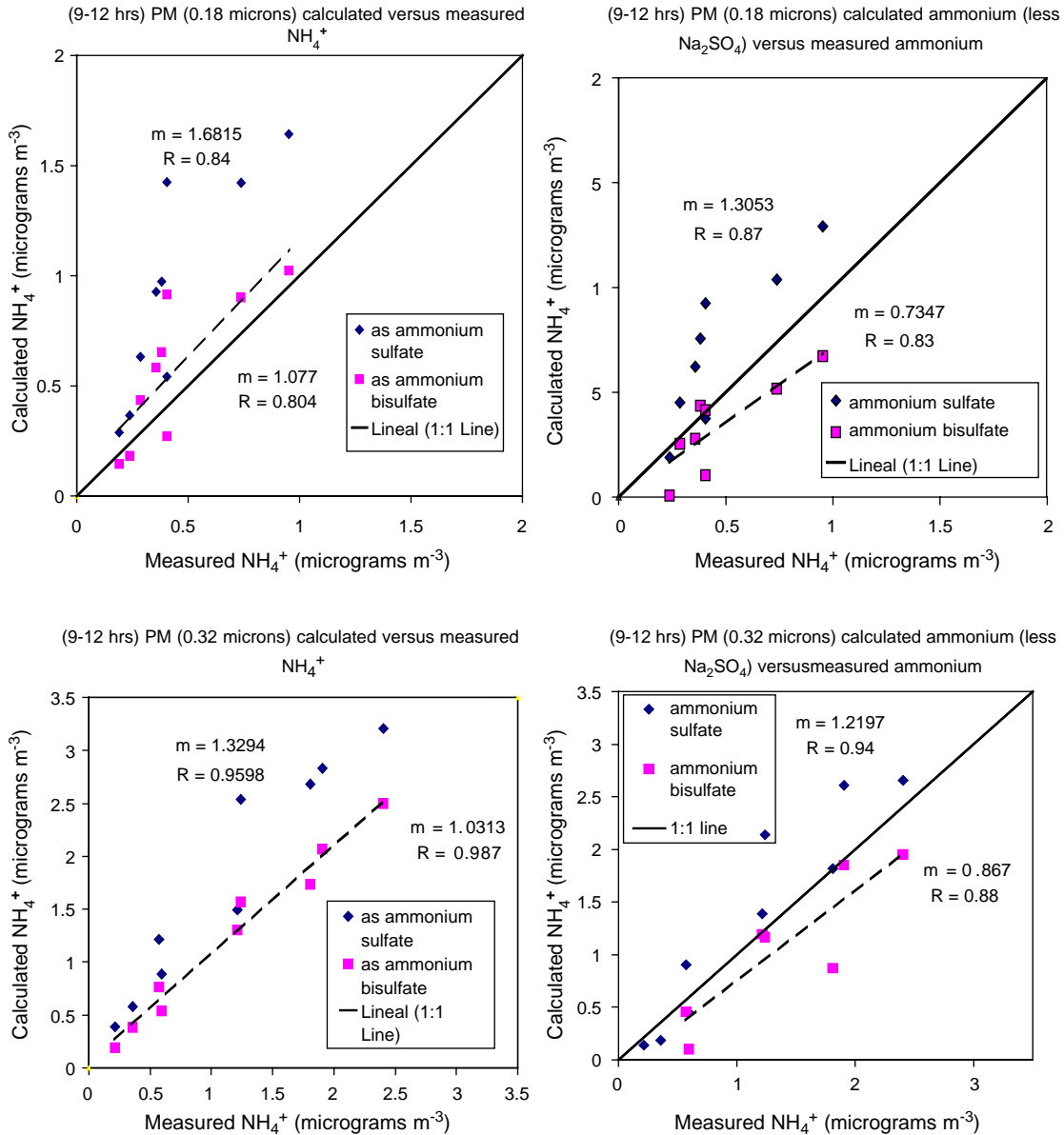


Fig. 8. Ammonium balances for the 1st and 2nd examples.

4. Conclusions

Measurements of size-differentiated inorganic aerosol particles and gas-phase precursors collected during January and February of 2003 at a site near downtown Mexico City have provided a wealth of information regarding the diurnal variability and partition of inorganic species between the gas and particulate phases. A bimodal inorganic aerosol distribution, typical of urban areas, was observed during all the sampling periods of the study. A more predominant mode was

observed over the accumulation size range during the morning sampling periods and over both accumulation and coarse modes during the afternoon sampling periods. Chloride and sodium were the dominant anion/cation over all of the sampling periods of the study. Ion balances applied over part of the samples collected over the accumulation mode showed sodium concentrations were combined with other anions, besides chloride, such as sulfate. With regards to coarse mode particles, the significant presence of sodium and the unexpected concentrations of crustals were explained

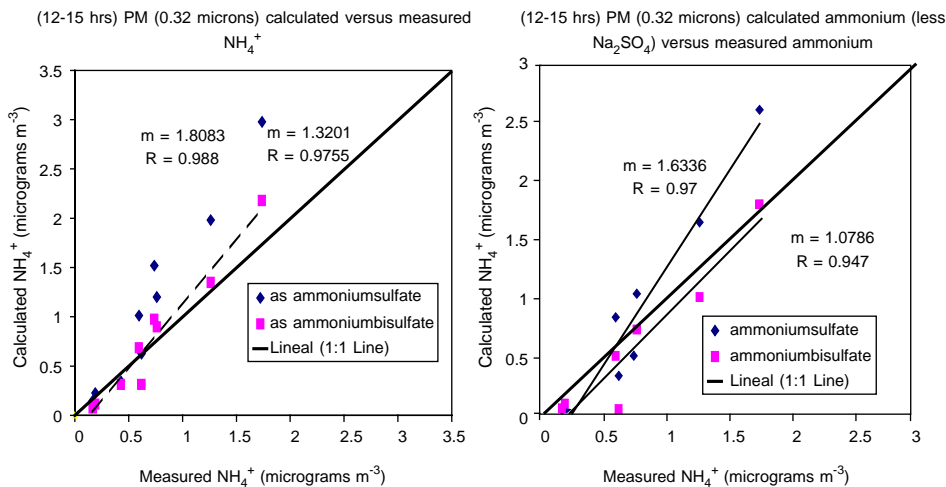


Fig. 9. Ammonium balances for the 3rd example.

in terms of the potential influence of the dry salt-lake of Texcoco, which is located towards the most prominent wind direction (~ 15 km to the NE of the sampling site) and resuspended dust/soil. Based on the analysis of the time-resolved gas-phase and PM composition, the significant presence of NH_3 during the 1st sampling periods had an important neutralizing effect on aerosol particles. This neutralization process is favored with lower temperatures and higher relative humidity values as were seen during the individual days of the campaign. Correlations of NH_4^+ in the accumulation mode with the gas-phase precursors (NH_3 and HNO_3) presented an inverse relation suggesting the gas-phase to PM conversion particularly during the late morning sampling periods.

Acknowledgements

The authors express their appreciation to R. Garcia, M.C. Torres, R. Belmont and H. Padilla for their collaboration in the analysis for inorganic ions, to T. Castro and C. Marquez for helping setting up the equipment at the measuring site and to M. Saavedra for helping in the conditioning of the filters. M. Grutter is grateful for the financial support of CONACyT through project J33620-T.M. Moya was supported in this project by the PAPIIT-UNAM grants IN117903-2 and IX116004.

References

- Chang, M.C., Sioutas, C., Kim, S., Gong Jr., Linn, W.S., 2000. Reduction of nitrate losses from filter and impactor samplers by means of concentration enhancement. *Atmospheric Environment* 34, 85–89.
- Chow, J.C., Fujita, E.M., Watson, J.G., Lu, Z., Lawson, D.R., 1994. Evaluation of filter-based aerosol measurements during the 1987 Southern California Air Quality Study. *Environmental Monitoring and Assessment* 30, 49–80.
- Dentener, F.J., Carmichael, G.R., Zhang, Y., Lelieveld, J., Crutzen, P.J., 1996. Role of mineral aerosol as a reactive surface in the global troposphere. *Journal of Geophysical Research* 101 (22), 869–889.
- Dockery, D.W., Schwarz, J., Spengler, J.H., 1992. Air pollution and daily mortality; associations with particles and acid aerosols. *Environmental Research* 59, 362–373.
- Dockery, D.W., Pope, X., Xu, J.D., Spengler, J.H., Ware, M.E., Fay, B.G., Speizer, F.E., 1993. An association between air pollution and mortality in six US cities. *New England Journal of Medicine* 329, 1753–1759.
- Edgerton, S.A., Arriaga, J.L., Archuleta, J., Bian, X., Bossert, J.E., Chow, J.C., Coulter, R.L., Doran, J.C., Doskey, P.V., Elliot, S., Fast, J.D., Gaffney, J.S., Guzman, F., Hubbe, J.M., Lee, J.T., Malone, E.L., Marley, N.A., McNair, L.A., Neff, W., Ortiz, E., Petty, R., Ruiz, M., Shaw, W.J., Sosa, G., Vega, E., Watson, J.G., Whiteman, C.P., Zhong, S., 1999. Particulate Air pollution in Mexico City. A Collaborative Research Project. *Journal of the Air and Waste Management Association* 49, 1221–1229.
- Fridlind, A.M., Jacobson, M.Z., 2000. A study of gas-aerosol equilibrium and aerosol pH in the remote marine boundary layer during the First Aerosol Characterization Experiment (ACE 1). *Journal of Geophysical Research* 105 (D15) 19, 891–19, 904.
- Grutter, M., Flores, E., Basaldud, R., Ruiz-Suárez, L.G., 2003. Open-path FTIR spectroscopic studies of the trace gases over Mexico City. *Atmospheric and Oceanic Optics* 16, 232–236.
- INEGI, 2000. <http://www.demographia.com/db-mxcward.htm>
- Jacobson, M.Z., 1999. Studying the effects of calcium and magnesium on size-distributed nitrate and ammonium with EQUISOLV II. *Atmospheric Environment* 33, 3635–3649.

- Jacobson, M.Z., 2002. *Atmospheric Pollution: History, Science, and Regulation*. Cambridge University Press, United Kingdom.
- Jáuregui, E., 1989. The dust storms of Mexico City. *International Journal of Climatology* 9, 169–180.
- Jazcilevich, A., Fuentes, V., Jáuregui, E., Luna, E., 2000. Simulated urban climate response to historical land use modification in the basin of México. *Climate Change* 44, 515–536.
- Marple, V.A., Rubow K, L., Behm S, M., 1991. A micro orifice uniform deposit impactor (MOUDI): description, calibration, and use. *Aerosol Science and Technology* 14, 434–446.
- Moya, M., Ansari, A.S., Pandis, S.N., 2001. Partitioning of nitrate and ammonium between the gas and particulate phases during the 1997 IMADA-AVER study in Mexico city. *Atmospheric Environment* 35, 1791–1804.
- Moya, M., Pandis, S.N., Jacobson, M.Z., 2002a. Is the size distribution of urban aerosols determined by thermodynamic equilibrium? An application to Southern California. *Atmospheric Environment* 36, 2349–2365.
- Moya, M., Pandis, S.N., Jacobson, M.Z., Ansari, A., 2002b. Evaluating the “bulk” and size-resolved aerosol modeling approaches in Mexico City and Southern California. *Proceedings of the 2002 American Association for Aerosol Research Conference*. Charlotte, NC, USA.
- Moya, M., Avalos-Gonzalez, E., Baumgardner, D., 2002c. Predicting size-differentiated inorganic species for Mexico City conditions with SELIQUID. *Proceedings of the 2002 American Association for Aerosol Research Conference*. Charlotte, NC, USA.
- Moya, M., Castro, T., Zepeda, M., Baez, A., 2003. Characterization of size-differentiated inorganic composition of aerosols in Mexico City. *Atmospheric Environment* 37, 3581–3591.
- Molina, M., Molina, L., 2002. *Air Quality in the Mexico Megacity: an integrated assessment*. Kluwer Academic Publishers, Dordrecht.
- Rothman, L.S., Rinsland, C.P., Goldman, A., Massie, S.T., Edwards, D.P., Flaud, J.-M., Perrin, A., Camy-Peyret, C., Dana, V., Mandin, J.-Y., Schroeder, J., McCann, A., Gamache, R.R., Wattson, R.B., Yoshino, K., Chance, K.V., Jucks, K.W., Brown, L.R., Nemtchinov, V., Varanas, P., 1998. The HITRAN molecular spectroscopic database. *Journal of Quantitative Spectroscopy and Radiative Transfer* 60, 665–710.
- Schwartz, S.E., 1996. The whitehouse effect-short-wave radiative forcing of climate by anthropogenic aerosols: an overview. *Journal of Aerosol Science* 27, 359–382.
- Seinfeld, J.H., Pandis, S.N., 1998. *Atmospheric Chemistry and Physics: from air pollution to climate change*. Wiley, New York.
- Spengler, J.D., Brauer, M., Koutratis, P., 1990. Acid air and health. *Environmental Science and Technology* 24, 946–955.
- Vega, E., Mugica, V., Reyes, E., Sanchez, G., Chow, J.C., Watson, J.G., 2001. Chemical composition of fugitive dust emitters in Mexico City. *Atmospheric Environment* 35, 4033–4039.
- Wall, S.M., John, W., Ondo, J.L., 1988. Measurements of aerosol size distribution for nitrate and major ionic species. *Atmospheric Environment* 22, 1649–1656.